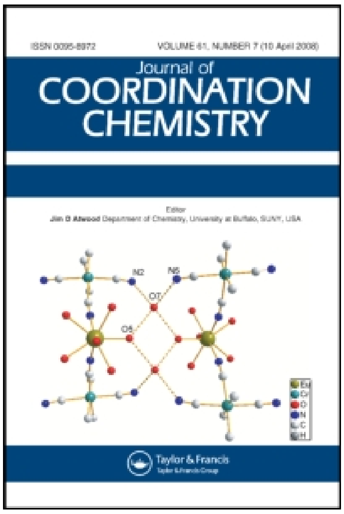

Journal of Coordination Chemistry
Publication details, including instructions for authors and subscription information:
http://www.informaworld.com/smpp/title~content=t713455674

Unexpected adduct formation in the reaction of peroxomonosulfate ion with the tris-(2,2'-bipyridine)iron(II) and tris-(1,10-phenanthroline)iron(II) complexes

Gábor Bellér[a]; Gabriella Bátki[a]; Gábor Lente[a]; István Fábián[a]
[a] Department of Inorganic and Analytical Chemistry, University of Debrecen, Debrecen 10, H-4010, Hungary

To cite this Article Bellér, Gábor , Bátki, Gabriella , Lente, Gábor and Fábián, István(2010) 'Unexpected adduct formation in the reaction of peroxomonosulfate ion with the tris-(2,2'-bipyridine)iron(II) and tris-(1,10-phenanthroline)iron(II) complexes', Journal of Coordination Chemistry, 63: 14, 2586 — 2597, First published on: 14 June 2010 (iFirst)

To link to this Article: DOI: 10.1080/00958972.2010.493213

URL: http://dx.doi.org/10.1080/00958972.2010.493213

Journal of Coordination Chemistry
Vol. 63, Nos. 14–16, 20 July–20 August 2010, 2586–2597

Unexpected adduct formation in the reaction of peroxomonosulfate ion with the tris-(2,2′-bipyridine)iron(II) and tris-(1,10-phenanthroline)iron(II) complexes

GÁBOR BELLÉR, GABRIELLA BÁTKI, GÁBOR LENTE
and ISTVÁN FÁBIÁN*

Department of Inorganic and Analytical Chemistry, University of Debrecen,
PO Box 21, Debrecen 10, H-4010 Hungary

(*Received 15 February 2010; in final form 30 March 2010*)

Formation of 1 : 1 adduct intermediates was detected between peroxomonosulfate ion and tris-(2,2′-bipyridine)iron(II) or tris-(1,10-phenanthroline)iron(II) complexes. The formation equilibrium constants were determined (27 ± 3 and $63 \pm 18\,(\mathrm{mol\,L^{-1}})^{-1}$) on the basis of kinetic measurements. The adduct was also detected by ESI mass spectrometry with the phenanthroline complex. A mechanism for the oxidation of tris-(2,2′-bipyridine)iron(II) or tris-(1,10-phenanthroline)iron(II) by peroxomonosulfate ion is proposed.

Keywords: Peroxomonosulfate ion; Fe(II) complexes; N-heteroaromatic ligands; Oxidation

1. Introduction

The iron(II) complexes of N-donor hetero-aromatic chelating ligands 2,2′-bipyridine (bipy) and 1,10-phenanthroline (phen) are easily prepared and widely used in numerous fields of chemistry as redox indicators and biologically-relevant model compounds [1–17]. These complexes, abbreviated as $\mathrm{Fe(bipy)_3^{2+}}$ and $\mathrm{Fe(phen)_3^{2+}}$ hereafter, have very intense red color with maximum molar absorption coefficients around $10^4\,(\mathrm{mol\,L^{-1}})^{-1}\,\mathrm{cm^{-1}}$ in the visible range. Their very high thermodynamic stability is primarily connected to a high-spin to low-spin transition in electronic structure during the stepwise complex formation between the bis and tris complexes [1, 6]. The widespread use of these compounds as redox indicators is due to the rather fast and reversible transformation to the corresponding blue-colored iron(III) complexes. The corresponding standard electrode potentials are 1.1 V [6], so it actually takes a strong oxidizing agent to prepare the iron(III) complexes. Lead(IV) oxide, chlorine, or cerium(IV) are suitable for this purpose, but certain peroxo-type oxidants also have the thermodynamic ability to oxidize $\mathrm{Fe(bipy)_3^{2+}}$ and $\mathrm{Fe(phen)_3^{2+}}$ [1, 18, 19].

Peroxomonosulfate ($\mathrm{HSO_5^-}$) is available in the form of a stable double salt, brand-named Oxone. It is a strong, two-electron oxidant and its reaction with $\mathrm{Fe(bipy)_3^{2+}}$ and

---

*Corresponding author. Email: ifabian@delfin.unideb.hu

Journal of Coordination Chemistry
ISSN 0095-8972 print/ISSN 1029-0389 online © 2010 Taylor & Francis
DOI: 10.1080/00958972.2010.493213

$Fe(phen)_3^{2+}$ should be interesting from a very fundamental kinetic point of view because the reactants are non-complementary and this fact makes the formation of a reactive sulfur intermediate very likely. Experiments in this system could add valuable information to the study of such sulfur intermediates and may clarify mechanistic assumptions in interpreting the autoxidation of sulfur(IV) [20]. In addition, valuable insight into the redox reactivity of biological model compounds can also be gained [6].

Some kinetic results on the reaction of HSO_5^- with both $Fe(bipy)_3^{2+}$ and $Fe(phen)_3^{2+}$ have already been published [21, 22]. However, our experiments failed to reproduce the findings reported in those works, both of which described very simple kinetic patterns. Our aim is to develop a coherent mechanism for these processes. In this study, a detailed kinetic model is proposed for the oxidation of $Fe(bipy)_3^{2+}$ and some of the basic differences between the reactions of the bipy and phen complexes are highlighted.

2. Experimental

2.1. *Materials*

Doubly-deionized and ultrafiltered water from a Millipore Q system was used to prepare the stock solutions and samples. Potassium peroxomonosulfate stock solutions were freshly prepared everyday from Oxone ($2KHSO_5 \cdot KHSO_4 \cdot K_2SO_4$, Aldrich) and standardized by iodometric titration. 1,10-Phenanthroline, 2,2′-bipyridine, $FeSO_4 \cdot 7H_2O$, H_2SO_4, and $Na_2SO_4 \cdot 10H_2O$ were commercial samples and used as received.

Iron(II) complexes were prepared by reacting concentrated solutions of bipy or phen and $FeSO_4 \cdot 7H_2O$ at controlled acidity. The solid complex was precipitated with a large excess of perchlorate ion from the concentrated solution. The product was soluble enough in pure water to prepare samples with concentration required in the kinetic experiments. The concentrations of these solutions were standardized by UV-Vis spectrophotometry using literature values for the molar absorption coefficients of both complexes: $\lambda_{max} = 522\,nm$ and $\varepsilon = 8.7 \times 10^3\,(mol\,L^{-1})^{-1}\,cm^{-1}$ for $Fe(bipy)_3^{2+}$ [5], $\lambda_{max} = 513\,nm$ and $\varepsilon = 1.1 \times 10^4\,(mol\,L^{-1})^{-1}\,cm^{-1}$ for $Fe(phen)_3^{2+}$ [10].

2.2. *Instrumentation and computation*

UV-Vis spectra and kinetic curves were recorded on Perkin Elmer Lambda 25 or Perkin Elmer Lambda 2S scanning, and HP-8543 diode-array spectrophotometers. Standard 1.000 cm cuvettes or two-chamber cells (0.846 cm) were used. Constant temperature (25.0 ± 0.1°C) was maintained in these experiments. The ionic strength was usually kept constant by using excess of sulfuric acid without additional salts. When pH dependences were studied, the constancy of the ionic strength was set with the addition of appropriate amounts of sodium sulfate. Electrospray ionization mass spectrometric (ESI–MS) analysis was carried out by a Bruker MicrOTOF-Q instrument in the positive ion mode. Non-linear least squares fitting was performed by the software Scientist [23].

3. Results

3.1. *Tris-(2,2′-bipyridine)iron(II)*

The spectral observations during the reaction between $Fe(bipy)_3^{2+}$ and HSO_5^- in sulfuric acid are shown in figure 1. The only clearly recognized effect is the disappearance of the red color of the initial iron(II) complex. To analyze the spectral changes further, we developed an absorbance-based graphic test that is able to distinguish composite processes from simple one-step reactions. A general reaction is represented as follows:

$$aA + bB \rightarrow cC + dD \tag{1}$$

It should be emphasized that the number of reactants and products and the stoichiometry are not limited to the ones shown in equation (1). If this is a one-step process, the concentrations of reactants and products can be given using a single time-function *f*(*t*):

$$\begin{aligned} [A] &= [A]_0 - af(t) \\ [B] &= [B]_0 - bf(t) \\ [C] &= [C]_0 + cf(t) \\ [D] &= [D]_0 + df(t) \end{aligned} \tag{2}$$

The absorbance at a given wavelength can be calculated after weighting with the appropriate molar absorption coefficients:

$$\begin{aligned} A(\lambda) &= \varepsilon_{A,\lambda}([A]_0 - af(t)) + \varepsilon_{B,\lambda}([B]_0 - bf(t)) \\ &\quad + \varepsilon_{C,\lambda}([C]_0 + cf(t)) + \varepsilon_{D,\lambda}([D]_0 + df(t)) \\ &= A_0(\lambda) - f(t)(a\varepsilon_{A,\lambda} + b\varepsilon_{B,\lambda} - c\varepsilon_{C,\lambda} - d\varepsilon_{D,\lambda}) \end{aligned} \tag{3}$$

The function *f*(*t*) can be given from equation (3) as follows:

$$f(t) = \frac{A_0(\lambda 1) - A(\lambda 1)}{a\varepsilon_{A,\lambda 1} + b\varepsilon_{B,\lambda 1} - c\varepsilon_{C,\lambda 1} - d\varepsilon_{D,\lambda 1}} \tag{4}$$

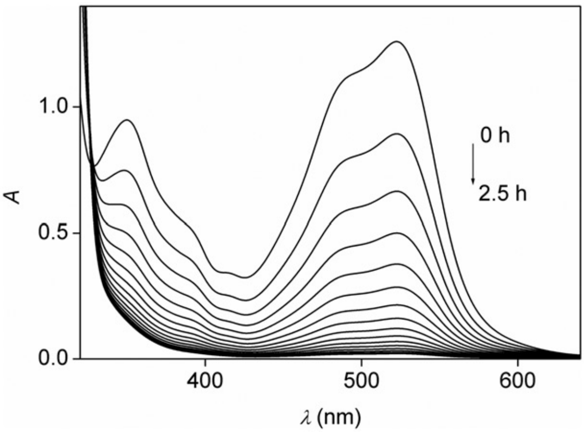

Figure 1. Spectral changes during the reaction between $Fe(bipy)_3^{2+}$ and HSO_5^-. $[HSO_5^-] = 5.0\,mmol\,L^{-1}$; $[Fe(bipy)_3^{2+}] = 0.22\,mmol\,L^{-1}$; $[H_2SO_4] = 0.10\,mol\,L^{-1}$; $T = 25.0°C$; path length, 0.846 cm; and cycle time, 10 min.

The absorbance at another wavelength can thus be given as

$$A(\lambda 2) = A_0(\lambda 2) - \frac{a\varepsilon_{A,\lambda 2} + b\varepsilon_{B,\lambda 2} - c\varepsilon_{C,\lambda 2} - d\varepsilon_{D,\lambda 2}}{a\varepsilon_{A,\lambda 1} + b\varepsilon_{B,\lambda 1} - c\varepsilon_{C,\lambda 1} - d\varepsilon_{D,\lambda 1}}(A_0(\lambda 1) - A(\lambda 1)) \tag{5}$$

Therefore, plotting the absorbance measured at one wavelength as a function of an absorbance measured at another wavelength at the same time should give a straight line for any one-step reaction (either going through the origin or with an intercept). This absorbance correlation test for the reaction between $Fe(bipy)_3^{2+}$ and HSO_5^- is shown with two pairs of wavelengths (490 *vs.* 520 nm and 350 *vs.* 520 nm) in figure 2. The 490–520 nm data give an excellent straight line. The 350–520 nm data also adhere reasonably to a straight line with an intercept, although a minor trend in the residual can also be seen on closer inspection. This could be indicative of an actual multistep process. However, the absorbance difference is very small, and the kinetic curves can be treated as those originating from a single-step reaction for all practical purposes. A possible reason for the minor deviation will be outlined in the discussion.

Detailed kinetic studies were carried out at the absorbance peak of $Fe(bipy)_3^{2+}$ at 520 nm using HSO_5^- in at least 10-fold (i.e., large) excess. A typical kinetic trace is shown in figure 3. In agreement with the one-step nature of the process, the kinetic curves could be fitted to exponential functions well. This means that pseudo-first-order conditions could be achieved [24]. Further support for this finding came from the fact that the pseudo-first-order rate constant showed the expected independence of the concentration of the limiting reagent $Fe(bipy)_3^{2+}$.

Figure 4 shows the dependence of the pseudo-first-order rate constant on the concentration of excess HSO_5^-. A saturation curve was revealed with an intercept. The intercept was confirmed experimentally in independent experiments using solutions not containing any oxidant. This intercept is due to the known acid dissociation of $Fe(bipy)_3^{2+}$ and will be discussed further.

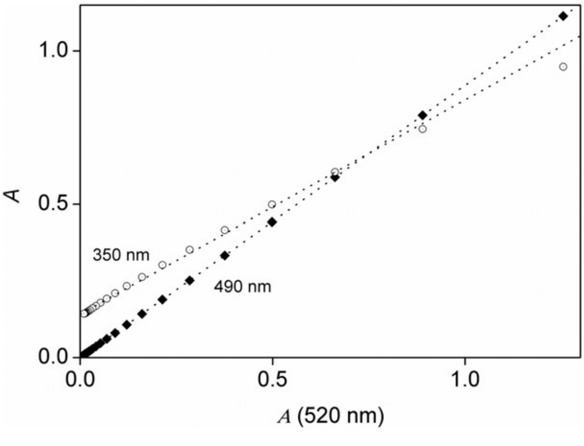

Figure 2. Absorbance correlation analysis for the reaction between $Fe(bipy)_3^{2+}$ and HSO_5^-. $[HSO_5^-] = 5.0\,mmol\,L^{-1}$; $[Fe(bipy)_3^{2+}] = 0.22\,mmol\,L^{-1}$; $[H_2SO_4] = 0.10\,mol\,L^{-1}$; $T = 25.0°C$; and path length, 0.846 cm.

Figure 5 shows that the addition of the free bipy had no influence on the kinetic curves. The experimentally measured rate constants were fitted to the following rate equation:

$$k_{\text{obs}} = \left(k_a + \frac{k_b[\text{HSO}_5^-]}{1 + K_c[\text{HSO}_5^-]} \right) \tag{6}$$

where non-linear least squares fitting gave $k_a = (3.35 \pm 0.05) \times 10^{-4}\,\text{s}^{-1}$, $k_b = (3.3 \pm 0.2) \times 10^{-2}\,(\text{mol L}^{-1})^{-1}\,\text{s}^{-1}$, and $K_c = 27 \pm 3\,(\text{mol L}^{-1})^{-1}$.

3.2. *Tris-(1,10-phenanthroline)iron(II)*

A characteristic kinetic trace measured in the $\text{Fe(phen)}_3^{2+}-\text{HSO}_5^-$ system is shown in figure 3. In this process, an initial decrease in absorbance is followed by a slow increase. This is an unquestionable evidence of a multistep process. This conclusion was further

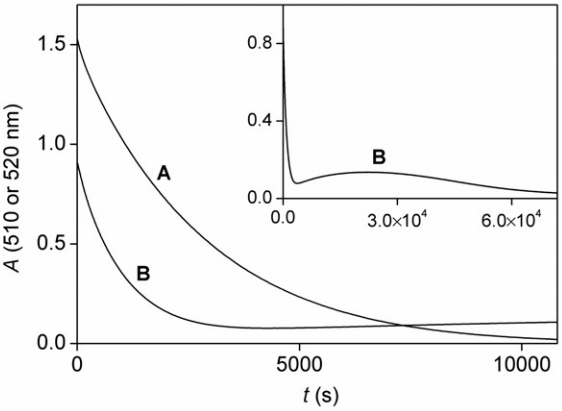

Figure 3. Kinetic traces obtained during oxidation of Fe(bipy)_3^{2+} (A) or Fe(phen)_3^{2+} (B) by HSO_5^-. $[\text{Fe(bipy)}_3^{2+}] = 0.22\,\text{mmol L}^{-1}$ (A); $[\text{Fe(phen)}_3^{2+}] = 0.081\,\text{mmol L}^{-1}$ (B); $[\text{HSO}_5^-] = 33\,\text{mmol L}^{-1}$ (A) and $30\,\text{mmol L}^{-1}$ (B); $[\text{H}_2\text{SO}_4] = 0.10\,\text{mol L}^{-1}$ (A) and $8.5\,\text{mmol L}^{-1}$ (B); $T = 25.0°\text{C}$; $\lambda = 520\,\text{nm}$ (A) and 510 nm (B); and path length, 0.846 cm (A), 1.000 cm (B). Inset, curve B on longer time scale.

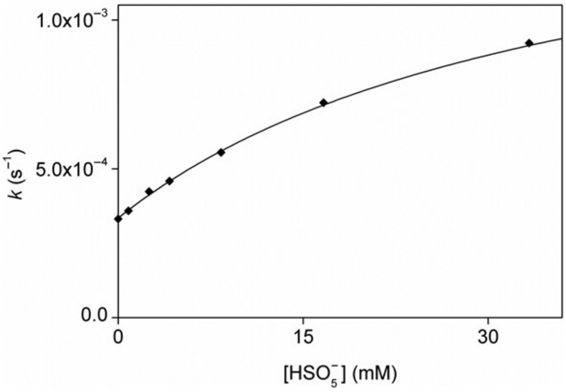

Figure 4. Dependence of the pseudo-first-order rate constant on HSO_5^- concentration during the reaction between Fe(bipy)_3^{2+} and HSO_5^-.
$[\text{Fe(bipy)}_3^{2+}] = 0.22\,\text{mmol L}^{-1}$; $[\text{H}_2\text{SO}_4] = 0.10\,\text{mol L}^{-1}$; $T = 25.0°\text{C}$.

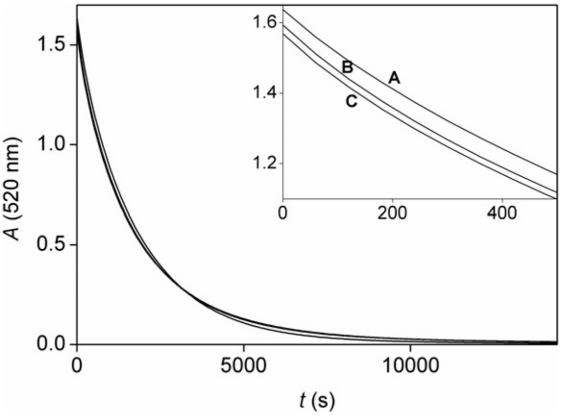

Figure 5. Effect of the addition of free 2,2′-bipyridine on the reaction between $Fe(bipy)_3^{2+}$ and HSO_5^-. $[Fe(bipy)_3^{2+}] = 0.22\,mmol\,L^{-1}$; $[HSO_5^-] = 8.33\,mmol\,L^{-1}$; $[H_2SO_4] = 0.10\,mol\,L^{-1}$; [bipy] = 0 (A) and $0.78\,mmol\,L^{-1}$ (B) and $1.56\,mmol\,L^{-1}$ (C); $T = 25.0°C$; and path length, 0.846 cm.

strengthened by the spectral observations which showed an isosbestic point at early reaction times (<1 h), which disappeared on a longer time scale. An earlier communication from our group [17] focusing primarily on the reactions of the iron(III) complex ferriin, $Fe(phen)_3^{3+}$, pointed out that a maximum also follows the minimum on this curve. An autocatalytic reaction of 1,10-phenanthroline-mono-N-oxide might be responsible for this unusual feature [17]. In this work, we focus on the reaction between $Fe(phen)_3^{2+}$ and HSO_5^-, which is not separated in time from subsequent reactions. Therefore, the detected curves were not exponential and could not be evaluated based on pseudo-first-order fitting. The initial rate method was used instead, which is free from interference from later processes. The initial rate was defined in this work as the initial rate of absorbance change at 510 nm, which is characteristic of the loss of $Fe(phen)_3^{2+}$:

$$v_0 = -\frac{\mathrm{d}A(510\ \mathrm{nm})}{\mathrm{d}t} = -\varepsilon_{510\ \mathrm{nm}}\frac{\mathrm{d}\,[\mathrm{Fe(phen)}_3^{2+}]_T}{\mathrm{d}t} \tag{7}$$

Figure 6 shows the dependence of the initial rate on the concentration of HSO_5^-. The rates show saturation and a small intercept similarly to figure 4. The small intercept was experimentally confirmed again in oxidant-free solutions. The $Fe(phen)_3^{2+}$-dependence of the initial reaction rate was studied as depicted in figure 7. At high HSO_5^- concentrations, the rate varies linearly with $Fe(phen)_3^{2+}$ concentration (curve A). However, a similar graph at lower oxidant concentrations shows saturation in rate. In this case, there is no intercept as no reaction is possible without the presence of $Fe(phen)_3^{2+}$. Free phenanthroline added to the reaction mixture did not influence the rate, similarly to the reaction of the $Fe(bipy)_3^{2+}$ complex.

The rate equation used for fitting the experimental data is as follows:

$$\begin{aligned} v_0 &= \frac{k_d}{2}X + k_e([\mathrm{Fe(phen)}_3^{2+}]_0 - X) \\ X &= Y - \sqrt{Y^2 - 4 \times [\mathrm{Fe(phen)}_3^{2+}]_0 \times [\mathrm{HSO}_5^-]_0} \\ Y &= [\mathrm{Fe(phen)}_3^{2+}]_0 + [\mathrm{HSO}_5^-]_0 + \frac{1}{K_f} \end{aligned} \tag{8}$$

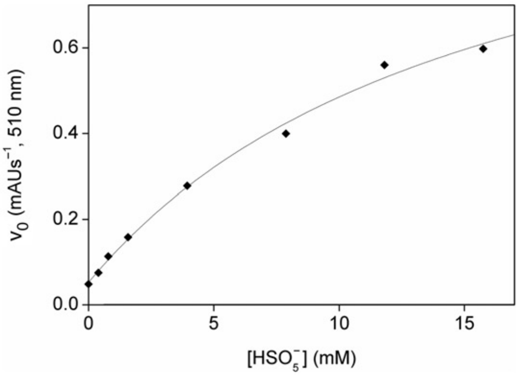

Figure 6. Dependence of the initial rate on HSO_5^- concentration during the reaction between $Fe(phen)_3^{2+}$ and HSO_5^-.
[$Fe(phen)_3^{2+}$] = 81 µmol L^{-1}; [H_2SO_4] = 8.5 mmol L^{-1}; $T = 25.0$°C; and path length, 1.000 cm.

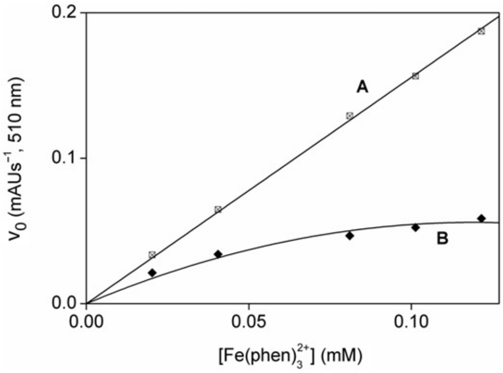

Figure 7. Dependence of the initial rate on $Fe(phen)_3^{2+}$ concentration during the reaction between $Fe(phen)_3^{2+}$ and HSO_5^-.
[HSO_5^-] = 1.67 mmol L^{-1} (A) and 93 µmol L^{-1} (B); [H_2SO_4] = 75 mmol L^{-1}; $T = 25.0$°C; and path length, 1.000 cm.

where the parameters $k_d = (1.3 \pm 0.2) \times 10^{-3}\,s^{-1}$, $k_e = (5.8 \pm 1.3) \times 10^{-5}\,s^{-1}$, and $K_f = 63 \pm 18\,(mol\,L^{-1})^{-1}$ were determined by non-linear least squares fitting.

Finally, the reaction mixture after about 5 min of reaction time was analyzed with ESI–MS. Figure 8 shows a part of the ESI–MS spectrum, which is characteristic of the formula $FeC_{36}H_{25}N_6O_5S^+$, equivalent to a direct adduct formed from $Fe(phen)_3^{2+}$ and HSO_5^-. This observation will be discussed later.

4. Discussion

All of our findings in the two different systems can be interpreted with the following common kinetic model:

$$\begin{gathered} Fe(N{-}N)_3^{2+}(+3H^+) \rightarrow Fe^{2+} + 3N{-}NH^+ \\ v = k_9[Fe(N{-}N)_3^{2+}] \end{gathered} \qquad (9)$$

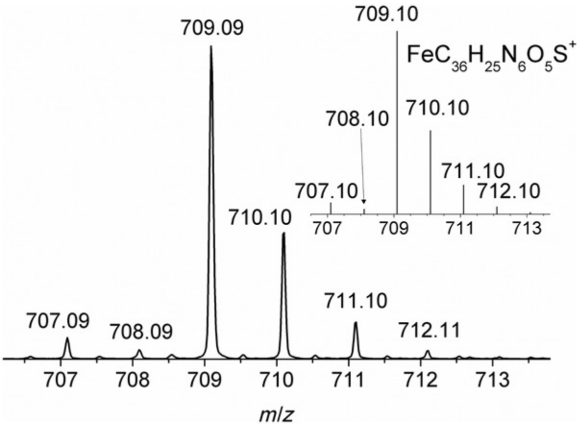

Figure 8. ESI–MS identification of the adduct in the reaction between Fe(phen)$_3^{2+}$ and HSO_5^-.
Notes: Inset, theoretically calculated spectrum for the formula $FeC_{36}H_{25}N_6O_5S^+$.

$$\begin{gathered}\mathrm{Fe(N{-}N)_3^{3+}(+3H^+)} \rightarrow \mathrm{Fe^{3+} + 3N{-}NH^+} \\ v = k_{10}[\mathrm{Fe(N{-}N)_3^{3+}}]\end{gathered} \tag{10}$$

$$\begin{gathered}\mathrm{Fe(N{-}N)_3^{2+} + HSO_5^-} \rightleftharpoons \mathrm{Fe(N{-}N)_3^{2+} \cdot HSO_5^-} \\ K_{11} = \frac{[\mathrm{Fe(N{-}N)_3^{2+} \cdot HSO_5^-}]}{[\mathrm{Fe(N{-}N)_3^{2+}}][\mathrm{HSO_5^-}]}\end{gathered} \tag{11}$$

$$\begin{gathered}\mathrm{Fe(N{-}N)_3^{2+} \cdot HSO_5^-(+H^+)} \rightarrow \mathrm{Fe(N{-}N)_3^{3+} + SO_4^- + H_2O} \\ v = k_{12}[\mathrm{Fe(N{-}N)_3^{2+} \cdot HSO_5^-}]\end{gathered} \tag{12}$$

$$\begin{gathered}\mathrm{Fe(N{-}N)_3^{2+} + SO_4^-} \rightarrow \mathrm{Fe(N{-}N)_3^{3+} + SO_4^{2-}} \\ v = \mathrm{fast}\end{gathered} \tag{13}$$

$$\begin{gathered}\mathrm{2Fe^{2+} + HSO_5^-(+H^+)} \rightarrow \mathrm{2Fe^{3+} + H_2O + SO_4^{2-}} \\ v = \mathrm{fast}\end{gathered} \tag{14}$$

This scheme is in agreement with the experimentally observed rate equations given in equations (6) and (8). Earlier, reaction (14) was confirmed to be fast on the time scale of this study [25]. The connection between the scheme in equations (9)–(14) and the parameters in experimentally established rate equations is as follows: $k_9 = k_a$, $K_{11} = K_c$, $k_{12} = k_b/K_c$ for Fe(bipy)$_3^{2+}$, and $k_9 = k_e$, $K_{11} = K_f$, $k_{12} = k_d$ for Fe(phen)$_3^{2+}$.

The parameters obtained from this study are collected in table 1 for both systems. The basic characteristics of these reactions can be demonstrated by the values shown. In the Fe(bipy)$_3^{2+}$ system, a single reaction is monitored that is basically the oxidation of Fe(bipy)$_3^{2+}$ to Fe(bipy)$_3^{3+}$. Dissociation of the product iron(III) complex is slower than the reaction monitored, but not by orders of magnitude. This slow subsequent minor dissociation could be the reason why a slight deviation from linearity is observed at the

Table 1. Parameters determined in the two reactions.

	$Fe(bipy)_3^{2+}$	$Fe(phen)_3^{2+}$
k_9	$(3.35 \pm 0.05) \times 10^{-4}\,s^{-1}$ (pH = 1)	$(5.8 \pm 1.3) \times 10^{-5}\,s^{-1}$ (pH = 2)
k_9 (literature)	$4.7 \times 10^{-4}\,s^{-1}$ (pH = 0.6) [2]	$7.5 \times 10^{-5}\,s^{-1}$ (pH = 1) [3]
k_{10} (literature)	$7.2 \times 10^{-5}\,s^{-1}$ (pH = 1.0) [8]	$2.9 \times 10^{-5}\,s^{-1}$ (pH = 0.0) [17] $9.8 \times 10^{-5}\,s^{-1}$ (pH = 1.4) [3]
K_{11}	$27 \pm 3\,(mol\,L^{-1})^{-1}$	$63 \pm 18\,(mol\,L^{-1})^{-1}$
k_{12}	$(1.2 \pm 0.1) \times 10^{-3}\,s^{-1}$	$(1.3 \pm 0.2) \times 10^{-3}\,s^{-1}$

350−520 nm curve in figure 2. However, the experiments cannot provide much information on this process because the absorbance contribution of the $Fe(bipy)_3^{3+}$ is low and the time scale of the experiments, designed to follow the redox reaction, is too short. The $Fe(phen)_3^{2+}$ reaction is much more complex as the oxidized free ligand (1,10-phenanthroline-mono-N-oxide) and its autocatalytic role become significant after about the first 30 min of the process [17]. The model proposed here, therefore, only interprets the initial part. It should be added that the pH dependence is not interpreted in detail here. Our measurements showed that varying the acidity did not change the kinetic curves much. In fact, this slight pH dependence could be interpreted by the known pH dependences of the k_9 values [2, 3, 5], which implies that only the acid dissociation of the iron(II) complexes shows pH-dependent kinetics, and not the oxidation reactions themselves. This is not unexpected as neither of the two reagents participate in any known pH-dependent equilibria in the concentration range of this study.

We would also like to comment on why our findings did not reproduce earlier published results. In the case of the reaction between $Fe(bipy)_3^{2+}$ and HSO_5^-, the earlier work was carried out between pH 4.6 and 9.0 [21]. First-order dependence for $Fe(bipy)_3^{2+}$ was observed similar to our results. No dependence on the oxidant concentration was reported (in contrast to the saturation kinetics observed here) and the added bipy decreased the reaction rate (in our experience, it has no influence). Unfortunately, no details were given in the earlier work beyond stating these facts. The significantly lower pH in our experiments (pH < 2) could account for the differences. The earlier work proposed a dissociative mechanism where the rate determining step is the dissociation of one bipyridine from $Fe(bipy)_3^{2+}$. This is clearly impossible under our conditions as the rate does depend on the oxidant concentration and cannot be inhibited by adding free ligand.

In the case of the reaction between $Fe(phen)_3^{2+}$ and HSO_5^-, the earlier study reported simple second-order kinetics in a pH range practically identical to ours [22]. The reaction was studied under pseudo-first-order conditions, and the multiphasic nature of the overall process was overlooked. A closer look at figure 1 in that work [22] reveals that kinetic curves were never monitored longer than two half lives and more than eight points per kinetic curve were never used. The serious shortcomings of this approach have been discussed in the chemical education literature, warning that it might very easily lead to invalid reaction orders [26–29]. So, the whole kinetic study [22] was based on a preconceived pseudo-first-order evaluation of kinetic curves that are, in fact, not exponential. In addition, the stoichiometric study reported there found a clear 2 : 1 ratio for the reactants, which seems highly questionable for several reasons. The experiments were carried out by using $Fe(phen)_3^{2+}$ in excess and determining its remaining concentration spectrophotometrically after the completion of the process. This is impossible because Fe(phen)$_3^{2+}$ is known to undergo acid dissociation on a time scale similar to the studied reaction itself [3]. In addition, our longer-scale kinetic curves clearly showed a multistep process, which has a complicated stoichiometry with the formation of 1,10-phenanthroline-mono-N-oxide, free phenanthroline, free iron(III) and, in the case of lower HSO_5^- concentrations, also free iron(II).

Amazingly, the formation of an adduct similar to the one shown in equation (11) was postulated in [22] despite the fact that the rate equation reported there did not require such an assumption. The experimental basis of this proposal was an observed small change in the UV-Vis spectra after mixing the reagents. We could not reproduce these observations. In fact, the unstructured small spectral changes (shown in the Supplementary information of [22]) may very well correspond to a shift in the spectral baseline. This effect could be tested based on the absorbance readings in regions where the solution does not absorb. However, this test is not possibly based on the published data as they were only given above the absorbance reading of 0.25.

The formation of adducts between HSO_5^- and coordinatively saturated Fe(bipy)$_3^{2+}$ or Fe(phen)$_3^{2+}$ might seem quite puzzling. There are two independent experimental findings that support this proposal: the rate equations found and the ESI–MS results.

The rate equations show that the reaction rate reaches a saturation value with increasing HSO_5^- concentration in both cases. In principle, a sequence of reactions where Fe(N$-$N)$_3^{2+}$ undergoes some oxidant-independent reaction first, the product of which reacts with HSO_5^- could also interpret such a saturation if there is a shift in the rate determining step. However, the dissociative pathway with an initial release of one ligand was explicitly ruled out in both the studied reactions. In addition, a dissociative mechanism like that would also contradict the saturation effect with increasing Fe(phen)$_3^{2+}$ concentration shown in figure 7. Therefore, association of reactants, i.e., adduct formation seems to be the simplest explanation which is in agreement with all experimental findings.

The ESI–MS spectrum shows high intensity peaks corresponding to the overall formula $FeC_{36}H_{25}N_6O_5S^+$. This formula clearly implies the existence of the adduct Fe(phen)$_3^{2+} \cdot HSO_5^-$. In principle, this does not necessarily mean that an adduct is present in the solution, it might only be formed in the mass spectrometer. However, this seems highly unlikely at the low operational pressure of the instrument. Additionally, the ion HSO_4^- is present at much higher concentration levels in the solution and would be expected to form such an adduct if the source were only the mass spectrometric technique itself. No peaks attributable to Fe(phen)$_3^{2+} \cdot HSO_4^-$ could be identified in the mass spectrum. Therefore, we conclude that the detected adduct must originate from the solution.

The nature of the adduct remains quite unclear at this point. It is unlikely to be a simple ion pair as the association constants (K_{11}) are about an order of magnitude higher than expected from the Fuoss equation for a $+2:-1$ ion pair ($K_{OS} = 5.2\,(\mathrm{mol\,L^{-1}})^{-1}$) [30]. Yet the UV-Vis spectra of the adducts seem to be indistinguishable from those of the parent complexes. Therefore, the coordination environment in the unassociated complexes must be identical to those in the adducts. It is also to be noted that the two different adducts decay with essentially the same first-order rate constant despite a significantly different association constant. This might be due to the fact that the aromatic pi electron systems are quite similar in the two ligands and the complexes; therefore, electron transfer with the oxidizing agent occurs with a very similar rate. This leads one to envisage some sort of interaction between the aromatic electron cloud and HSO_5^- as the driving force of adduct formation, but any such proposal would be highly speculative.

5. Conclusion

We have detected the formation of unexpected adducts between HSO_5^- and $Fe(bipy)_3^{2+}$ or $Fe(phen)_3^{2+}$. The formation equilibrium constants were determined and in the case of the $Fe(phen)_3^{2+}$ system, the adduct was also detected by ESI–MS. The adduct formation is the only pathway for the redox reaction between the two reactants.

Acknowledgments

The authors thank the Hungarian Science Foundation for financial support under grant nos. K68668 and K77936. Dr János Török and Dr Lajos Nagy are gratefully acknowledged for assistance in the ESI–MS measurements.

References

[1] T.S. Lee, I.M. Kolthoff, D.L. Leussing. *J. Am. Chem. Soc.*, **70**, 2348 (1948).
[2] F. Basolo, J.C. Hayes, H.M. Neumann. *J. Am. Chem. Soc.*, **76**, 3807 (1954).
[3] J.E. Dickens, F. Basolo, H.M. Neumann. *J. Am. Chem. Soc.*, **79**, 1286 (1957).
[4] D.W. Margerum. *J. Am. Chem. Soc.*, **79**, 2728 (1957).
[5] E.A. Healy, R.K. Murmann. *J. Am. Chem. Soc.*, **79**, 5827 (1957).
[6] B.R. James, J.R. Lyons, R.J.P. Williams. *Biochemistry*, **1**, 379 (1962).
[7] G. Nord, T. Pizzino. *Chem. Commun.*, 1633 (1970).
[8] G. Nord, B. Pedersen, E. Bjergbakke. *J. Am. Chem. Soc.*, **105**, 1913 (1983).
[9] K. Arora, A.P. Bhargava, Y.K. Gupta. *J. Chem. Soc. Dalton Trans.*, 1257 (1990).
[10] S. Kéki, I. Magyar, M.T. Beck, V. Gáspár. *J. Phys. Chem.*, **96**, 1725 (1992).
[11] K. Sriramam, C. Ramakrishna, J. Sreelakshmi. *React. Kinet. Catal. Lett.*, **61**, 209 (1997).
[12] J. Wang, J. Zhao, Y. Chen, Q. Gao, Y. Wang. *J. Phys. Chem. A*, **109**, 1374 (2005).
[13] L. Hegedűs, H.D. Försterling, L. Onel, M. Wittmann, Z. Noszticzius. *J. Phys. Chem. A*, **110**, 12839 (2006).
[14] R.K. Adhikamsetty, N.R. Gollapalli, S.B. Jonnalagadda. *Int. J. Chem. Kinet.*, **40**, 515 (2008).
[15] N. Li, J. Wang. *J. Phys. Chem. A*, **113**, 6297 (2009).
[16] G. Accorsi, A. Listorti, K. Yoosaf, N. Armaroli. *Chem. Soc. Rev.*, **38**, 1690 (2009).
[17] G. Bellér, G. Lente, I. Fábián. *Inorg. Chem.*, **49**, 3968 (2010).
[18] G. Nord, O. Wernberg. *J. Chem. Soc. Dalton Trans.*, 866 (1972) and references therein.
[19] G. Nord, O. Wernberg. *J. Chem. Soc. Dalton Trans.*, 845 (1975) and references therein.
[20] I. Kerezsi, G. Lente, I. Fábián. *Dalton Trans.*, 955 (2006).
[21] R. Somuthevan, R. Renganathan, P. Maruthamuthu. *Inorg. Chim. Acta*, **45**, L165 (1980).
[22] M. Mehrotra, R.N. Mehrotra. *Polyhedron*, **27**, 2151 (2008).
[23] *SCIENTIST (Version 2.0)*, Micromath Software, Salt Lake City, Utah, USA (1995).
[24] J.H. Espenson. *Chemical Kinetics and Reaction Mechanisms*, 2nd Edn, McGraw-Hill, New York, USA (1995).
[25] G. Lente, J. Kalmár, Zs. Baranyai, A. Kun, I. Kék, D. Bajusz, M. Takács, L. Veres, I. Fábián. *Inorg. Chem.*, **48**, 1763 (2009).

[26] E.T. Urbansky. *J. Chem. Educ.*, **78**, 921 (2001).
[27] G. Lente. *J. Chem. Educ.*, **81**, 32 (2004).
[28] S. Le Vent. *J. Chem. Educ.*, **81**, 32 (2004).
[29] E.T. Urbansky. *J. Chem. Educ.*, **81**, 32 (2004).
[30] R.M. Fuoss. *J. Am. Chem. Soc.*, **80**, 5059 (1958).